



High-resolution $^{40}\text{Ar}/^{39}\text{Ar}$ dating of the oldest oceanic basement basalts in the western Pacific basin

Anthony A. P. Koppers and Hubert Staudigel

Institute of Geophysics and Planetary Physics, Scripps Institution of Oceanography, University of California, San Diego, La Jolla, California 92093-0225, USA (akoppers@ucsd.edu)

Robert A. Duncan

College of Oceanic and Atmospheric Sciences, Oregon State University, 104 Ocean Administration Building, Corvallis, Oregon 97331-5503, USA

[1] We report new $^{40}\text{Ar}/^{39}\text{Ar}$ ages for the oldest Pacific oceanic floor at Ocean Drilling Program Site 801C in the Pigafetta basin and Site 1149D close to the Izu-Bonin subduction zone in the Nadezhda basin. These ages were determined by applying high-resolution incremental heating experiments (including 15–30 heating steps) to better resolve the primary argon signal from interfering alteration signatures in these low-potassium ocean crust basalts. Combined with previous results from Pringle [1992] for Site 801B and 801C, we arrive at a multistage history for the formation of the Pigafetta ocean crust. The oldest part of the Pacific plate was formed at the spreading ridges at $167.4 \pm 1.4/3.4$ Ma ($n = 2$, 2σ internal/absolute error), offering an important calibration point on the Geological Reversal Timescale (GRTS) since it represents the old end of the Mesozoic magnetic anomalies. This mid-ocean ridge basalt sequence, however, is overlain by more tholeiites and alkali basalts that were formed 7.3 ± 1.5 Myr later around 160.1 ± 0.6 Ma ($n = 7$, 2σ internal error). The older age group is confirmed independently by radiolarian ages ranging from Late Bajocian to Middle Bathonian (167–173 Ma [Bartolini and Larson, 2001]) and by profound differences in the structural characteristics of this basement section [Pockalny and Larson, 2003]. Thin layers comprising hydrothermal deposits separate these sequences, which in addition to the difference in isotopic age show distinct major and trace element compositions. This indicates that key volcanic and hydrothermal activity took place 400–600 km away from the spreading ridges, on the basis of a Jurassic ~ 66 km/Myr half spreading rate in the Pacific. It remains unclear if these processes were active continuously after the initial formation of the Pacific oceanic crust, but all our observations seem to point to an episodic history. Site 1149D gives another important calibration point on the GRTS of $127.0 \pm 1.5/3.6$ Ma ($n = 1$, 2σ internal/absolute error) for anomaly M12 that is slightly younger when compared to current timescale compilations (134.2 ± 2.1 Ma [Gradstein et al., 1995]). This might suggest that the dated basalt from Site 1149D does not represent the age of the ocean crust formed at its ridge axis; it may also be part of the Early Cretaceous intraplate events that have produced dolerite sills in the Pacific crust at Sites 800 and 802 around 114–126 Ma.

Components: 10,717 words, 4 figures, 4 tables.

Keywords: $^{40}\text{Ar}/^{39}\text{Ar}$ geochronology; oceanic basement; submarine alteration; Pacific plate; subduction; standard geological timescale.

Index Terms: 1035 Geochemistry: Geochronology; 9604 Information Related to Geologic Time: Cenozoic; 3035 Marine Geology and Geophysics: Mid-ocean ridge processes.

Received 5 May 2003; **Revised** 24 September 2003; **Accepted** 26 September 2003; **Published** 25 November 2003.

Koppers, A. A. P., H. Staudigel, and R. A. Duncan, High-resolution ⁴⁰Ar/³⁹Ar dating of the oldest oceanic basement basalts in the western Pacific basin, *Geochem. Geophys. Geosyst.*, 4(11), 8914, doi:10.1029/2003GC000574, 2003.

Theme: Oceanic Inputs to the Subduction Factory

Guest Editors: Terry Plank and John Ludden

1. Introduction

[2] Ocean Drilling Program (ODP) Sites 801 and 1149 were drilled in the Pacific plate (Figure 1) of Middle Jurassic and Early Cretaceous age, representing the oldest intact oceanic basement still present on the Earth's surface. Both drill sites form key calibration points for the M-series reversals and hence the Geological Reversal Timescale (GRTS). Site 801 is located in the Jurassic Quiet Zone (JQZ) of the Pigafetta basin only about 450 km away from Mesozoic magnetic anomaly M35, whereas Site 1149 is located on top of anomaly M12 in the Nadezhda basin (Figure 1). High-resolution ⁴⁰Ar/³⁹Ar isotopic dating is required to achieve an improved calibration of the GRTS and this part of the Pacific plate gives an unique opportunity to accomplish this, because of its "superfast" spreading (~80 km/Myr, half-rate [Pockalny and Larson, 2003]) during the Jurassic and Early Cretaceous, leveraging more accurate calibration results due to an increased geospatial resolution.

[3] Previous ⁴⁰Ar/³⁹Ar age determinations were published by Pringle [1992] on the basis of the first entry of the 801C drill hole that penetrated 131 m of basaltic basement [Lancelot *et al.*, 1990]. The upper part of this Jurassic basement can be divided into a sequence of alkali basalts (Sequence I) and tholeiitic pillow basalts (Sequence III–IV), divided by a hydrothermal horizon that is ~20 m thick (Sequence II; Figure 3). Pringle showed that the alkali basalts (157.4 ± 0.5 Ma, 1σ and *n* = 5) are decidedly younger than the underlying tholeiitic basalts (166.8 ± 4.5 Ma, 1σ and *n* = 2). He also noted the close coincidence of the older 166.8 Ma age with extrapolations based on the M-series magnetic anomalies and the Harland *et al.* [1990] timescale. However, the large error bar (even at the 1σ confidence level) renders this age result not

practical for calibration purposes. This is even more so, because the 166.8 ± 4.5 Ma age result is an weighted average of two independent age determinations that are significantly different at the 95% confidence level (158.6 ± 5.4 Ma, 2σ and 171.5 ± 2.2 Ma, 2σ; Pringle, 1992) and because it is an internal ⁴⁰Ar/³⁹Ar age that does not include error contributions from the ⁴⁰K → ⁴⁰Ar decay constant and standard calibrations.

[4] During ODP Leg 185 [Plank *et al.*, 2000] Site 801C was deepened by another 359 m giving us the possibility to better determine the age characteristics of the oldest oceanic crust in the Pacific basin. The deeper part of the 801 basement site continues the sequence of tholeiitic pillow basalts (Sequence IV) and can be further divided into a sequence of massive basaltic flows (Sequence VI) and tholeiitic pillow basalts (Sequence VIII; Figure 3). In these sections another hydrothermal layer is found at 625 mbsf (Sequence V) and a tectonic breccia (Sequence VII) is located between Sequence VI and VII. In this study, we expanded the ⁴⁰Ar/³⁹Ar age database by dating one sample from the "upper pillow basalts" and two samples from the "lower massive flows" (Figure 3). By applying high-resolution incremental heating experiments we could establish that a significant age difference of 7.3 ± 1.5 Myr exists (at the 95% confidence level) between the deeper part of the Pacific crust in the Pigafetta basin and the overlying pillow and alkali basalts. The 7.3 Myr age difference indicates that the upper 175 m of this oceanic crust was formed off-axis, as predicted by the fluctuating-magmatism accretion model [Hurst *et al.*, 1994; Karson *et al.*, 2002; Pockalny and Larson, 2003]. This makes the older 167.4 ± 3.4 Ma (*n* = 2, 2σ absolute error) basalt sequence coincident with the formation of the Pacific oceanic crust at its ridge and therefore should be used for the GRTS calibration. This scenario is reaffirmed by the age range

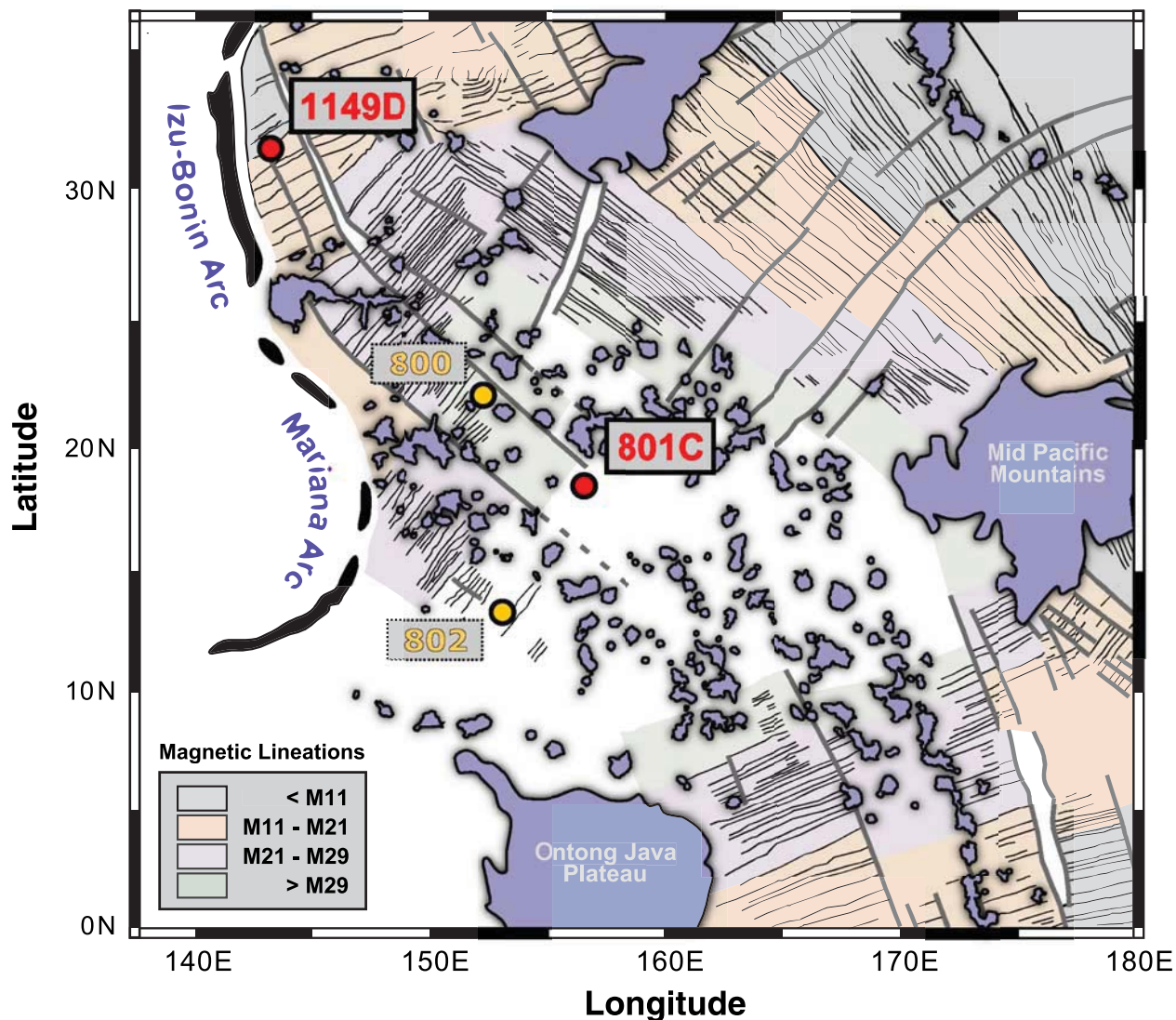


Figure 1. Location map of the West Pacific Seamount Province (WSP) with the locations of the ODP Leg 185 drill Sites 801C and 1149D. The Jurassic Geological Reversals [Cande and Kent, 1992] and fracture zones for the oceanic basement [Nakanishi et al., 1992; Abrams et al., 1993; Nakanishi, 1993] are shown for reference, as well as the location of ODP basement Sites 800 and 802 [Lancelot et al., 1990].

documented in the radiolarian record [Bartolini and Larson, 2001] that starts about 258 m deep into this basement with Late Bajocian species (173 Ma) and ends at the top of the basement with Middle Bathonian species (167 Ma).

[5] In this paper, we will present new high-resolution ⁴⁰Ar/³⁹Ar data for Sites 801C and 1149D and discuss the quality of these experiments in the light of the challenges of dating altered, low-potassium submarine basalts [cf. Koppers et al., 2000]. In addition, we will discuss the impact of using

realistic uncertainties for the decay constants, age standard inter-calibrations and other physical parameters on the ⁴⁰Ar/³⁹Ar age calculations [see also Renne et al., 1998; Min et al., 2000; Koppers, 2002]. To be able to use these ages in the calibration of the GRTS, we need to recalibrate the fundamentally relative ⁴⁰Ar/³⁹Ar ages toward a primary K-Ar dating standard (or an external age standard calibrated by other geochronological methods) and we need to include all (systematic) errors to come to the most accurate estimate for its absolute age uncertainties. For rocks of Jurassic

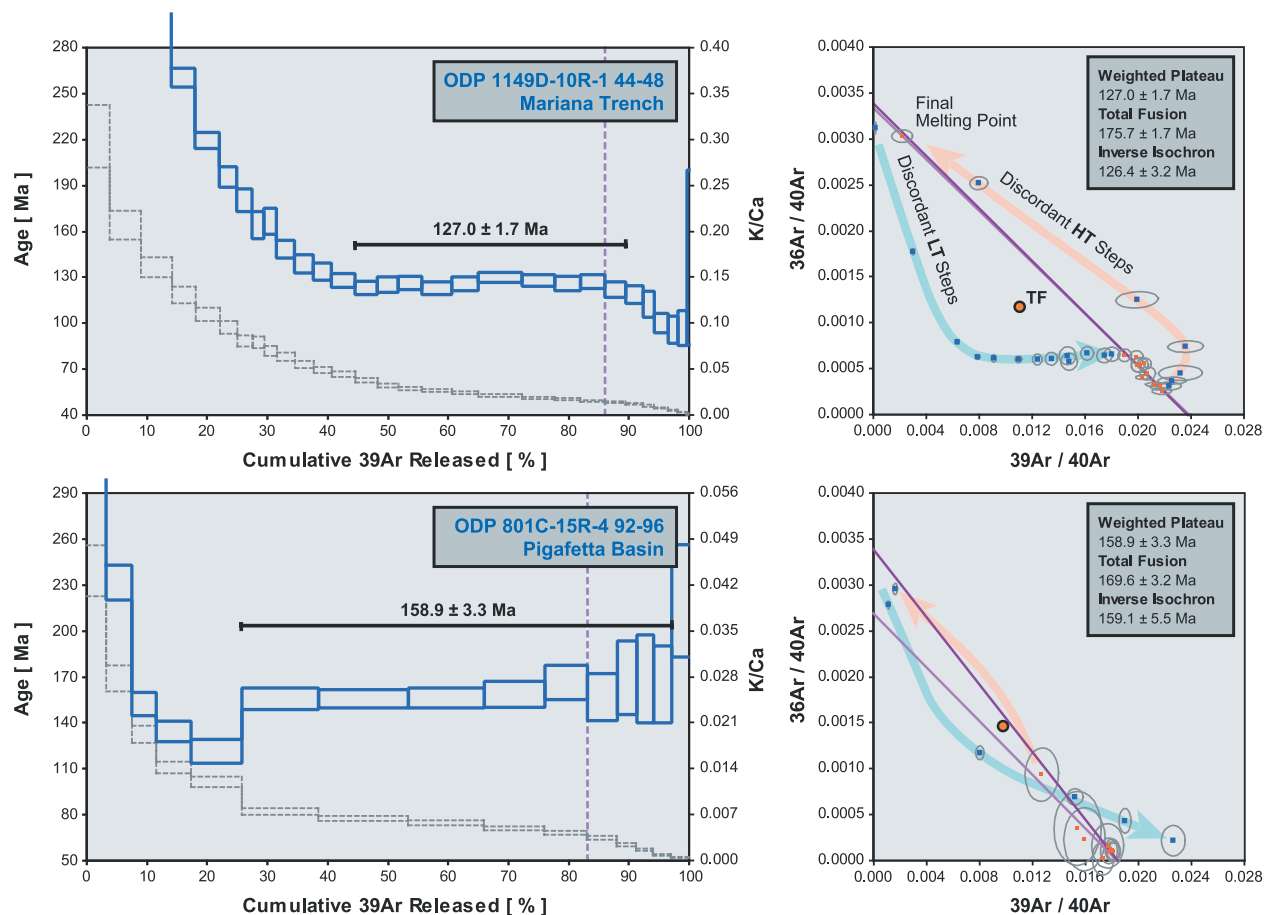


Figure 2. High-resolution incremental heating ⁴⁰Ar/³⁹Ar analyses for the Leg 185 basement basalts. The reported ⁴⁰Ar/³⁹Ar ages are weighted age estimates and errors on the 95% confidence level including 0.3–0.4% standard deviations in the J-value. All samples were monitored against FCT-3 biotite (28.04 Ma). Data are listed in Table 1 and ArArCALC age calculation files can be downloaded from the Table in Appendix A. Vertical lines represent the starting points of melt glazing that are associated with spikes in ³⁷Ar_{Ca} release.

and Cretaceous age these absolute errors may be up to three times higher than the internal ages that normally are being published in the case of ⁴⁰Ar/³⁹Ar dating [cf. *Min et al.*, 2000]. Only when including such a comprehensive error treatment and when calibrating the ages against a primary K-Ar age standard, we will be able to confidently and accurately compare the ⁴⁰Ar/³⁹Ar ages with other age estimates, such as derived by U-Pb mineral dating.

2. The ⁴⁰Ar/³⁹Ar Dating Techniques

[6] We analyzed four samples from ODP Drill Sites 801C ($n = 3$) and 1149D ($n = 1$) using ⁴⁰Ar/³⁹Ar incremental heating techniques. The data are

displayed in age plateau and isochron diagrams in Figure 2 and compiled in Table 1. Analytical data can be downloaded from the EarthRef.org Digital Archive (ERDA) as detailed in Appendix A.

[7] Incremental heating ⁴⁰Ar/³⁹Ar age determinations were performed on crystalline groundmass separates using a CO₂ laserprobe combined with a MAP-215/50 mass spectrometer at Oregon State University (Corvallis). Sample preparation and acid leaching are described in *Koppers et al.* [2000]. The mass spectrometer is a 90° sector instrument with a Nier-type source with an all-metal extraction system for ⁴⁰Ar/³⁹Ar age determinations. It has an electron multiplier for high sensitivity and an electrostatic analyzer with adjustable collector slit for an effective resolution

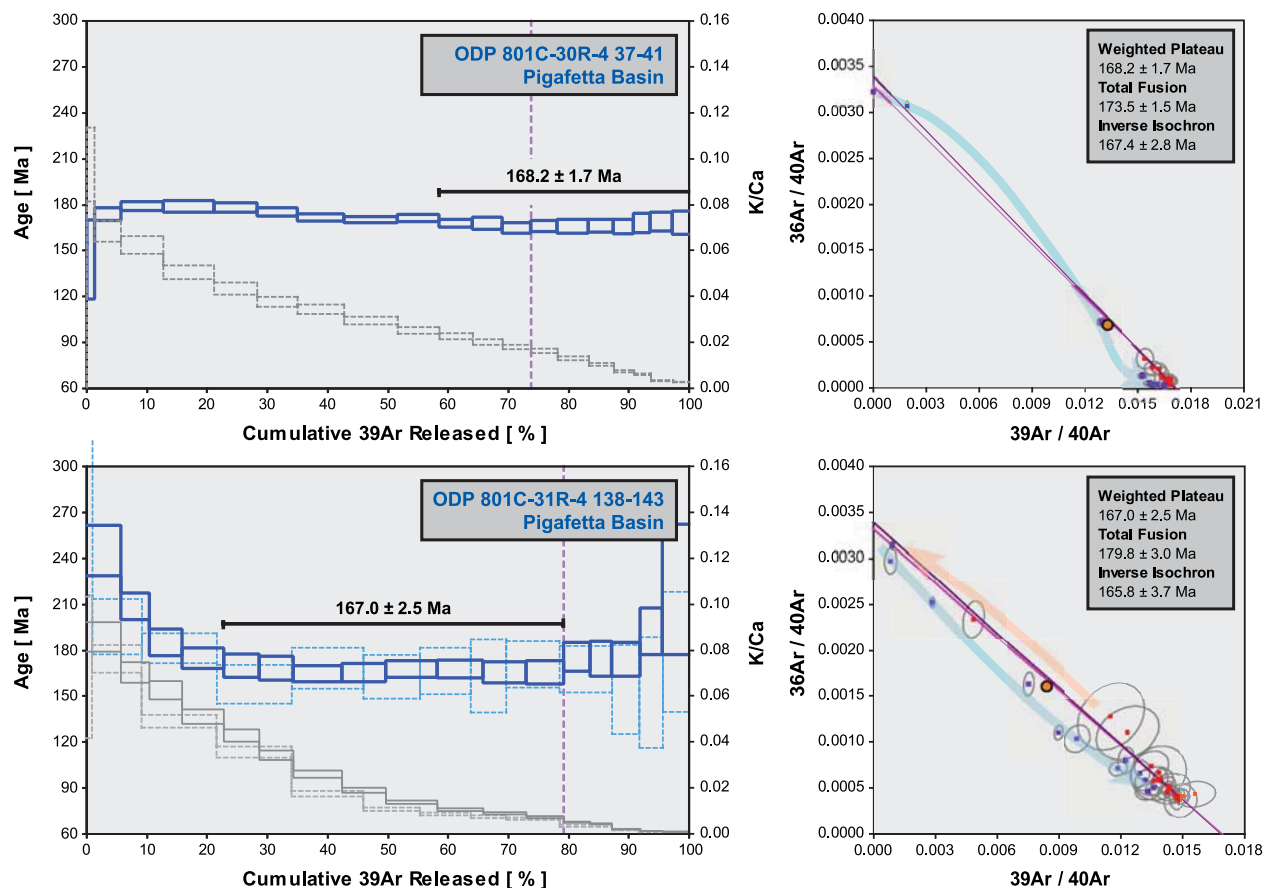


Figure 2. (continued)

(~600) of Ar peaks from small hydrocarbon peaks. For incremental heating the system is equipped with a Merchantek integrated CO₂ laser gas extraction system connected to an ultra-clean gas cleanup line (~1000 cc; Zr-Al getters). Irradiated ground-mass samples were loaded into Cu-planchettes designed with a variety of pans that hold up to 50 mg of material, which are then pumped within a sample chamber fitted with a ZnSe window transparent to the CO₂ laser wavelength. Software allows for scanning across samples in a preset pattern with a defocused beam, to evenly heat the material. Ion beam currents are measured with the electron multiplier at m/z = 35, 36, 37, 38, 39, 40 and intervening baselines with an 8.5 digit integrating HP multimeter. The multiplier is operating at 2050 Volt with a system sensitivity of 4×10^{-14} mol/volt. Peak decay is typically less than 10% during analyses and the regressed peak heights against time (normally) follow first-order

and second-order polynomial fits. The background for the mass spectrometer (subsequent to 20 min isolation from pumps) is 1×10^{-18} mol at m/z = 36, 2×10^{-18} mol at m/z = 39 and 2×10^{-16} mol at m/z = 40. The average extraction line blank is 4×10^{-19} mol at m/z = 36 and 2×10^{-16} mol at m/z = 40. Mass discrimination (1.0149 ± 0.0012 amu⁻¹) is monitored using zero age basaltic glass. Estimated uncertainties for the J-values are between 0.3–0.4% standard deviation. Sample irradiation was carried out using the TRIGA CLICIT at the OSU reactor facility for 6 hours.

[8] All new argon ages were measured relative to the flux monitor standard FCT-3 biotite (28.04 ± 0.18 Ma, 1σ [Renne *et al.*, 1994]) and the results of Pringle [1992] were recalibrated from the 27.92 Ma TCR standard to FCT-3 to allow for direct age comparison (Table 1). The final ages used in this paper (Table 3) have all been recal-

Table 1. Incremental Heating ⁴⁰Ar/³⁹Ar Analyses on Leg 185 Basement Basalts^a

Depth, mbsf	Sample Type	Study Identifier	Analysis Type	Age Spectrum			Total Fusion		Inverse Isochron Analyses				
				Age ± 2σ, Ma	³⁹ Ar, %	K/Ca	MSWD	n	Age ± 2σ, Ma	Age ± 2σ, Ma	⁴⁰ Ar/ ³⁶ Ar intercept	MSWD	
<i>Pigafeta Basin (Sites 801B and 801C), 18°38.538'N, 156°21.588'E</i>													
160.2 ± 0.7 [n = 5]													
Alkalic Basalts													
801C-01R-1 109-119	494	Plagioclase	DGAS + TF	MSP1992	160.0 ± 1.6	100	0.037	6	160.1 ± 1.6	158.5 ± 1.6	287.3 ± 35.2	0.4	
		Plagioclase	IHE	MSP1992	158.5 ± 1.6	98	0.051	8	158.7 ± 1.8	162.1 ± 4.1	313.9 ± 37.8	0.8	
		Biotite	DGAS + TF	MSP1992	163.9 ± 1.8	100	3.158	6	163.9 ± 1.8	160.5 ± 1.4	295.0 ± 8.6	0.3	
801B-44R-3 13-22	503	Plagioclase	DGAS + TF	MSP1992	160.5 ± 1.0	69	0.022	5	156.0 ± 2.8	156.4 ± 5.2	305.1 ± 53.6	0.1	
		Plagioclase	IHE	MSP1992	157.3 ± 2.0	50	0.022	4	150.6 ± 3.8				
Tholeiites: Upper Massive Flows and Pillow Basalts													
801C-10R-5 53-58	569	Basalt core	IHE	MSP1992	159.5 ± 2.8	[n = 2]	without 801C-10R-6 21-26	4	166.6 ± 4.0				
801C-10R-6 21-26	569	Basalt chips	DGAS + TF	MSP1992	161.0 ± 5.4	59	0.009	4	166.6 ± 4.0				
801C-15R-4 92-96	614	Groundmass	HR-IHE	K2003	174.1 ± 2.2	62	0.012	9	178.4 ± 2.2	175.6 ± 11	285.7 ± 61.8	1.6	
					158.9 ± 3.3	71	0.003	9	169.6 ± 3.2	159.1 ± 5.5	398.2 ± 102	0.9	
Tholeiites: Lower Massive Flows													
801C-30R-4 37-41	747	Groundmass	HR-IHE	K2003	167.7 ± 1.4	[n = 2]		10	173.5 ± 1.5	167.4 ± 2.8	343.1 ± 126	0.6	
801C-31R-4 138-143	757	Groundmass	HR-IHE	K2003	168.2 ± 1.7	41	0.004	10	172.1 ± 5.3	163.8 ± 7.0	308.2 ± 32.8	0.4	
		Repeat	HR-IHE	K2003	165.1 ± 5.5	78	0.002	5	179.8 ± 3.0	164.5 ± 15	326.1 ± 175	0.3	
			combined		167.0 ± 2.5	57	0.011	8	176.8 ± 2.6	165.8 ± 3.5	305.9 ± 31.2	0.4	
					166.7 ± 2.4	65	0.004	4					
<i>Mariana Trench (Site 1149D), 31°18.790' N, 143°24.030' E</i>													
127.1 ± 1.5 [n = 1]													
Basaltic Basement													
1149D-10R-1 44-48	350	Groundmass	HR-IHE	K2003	127.8 ± 8.4	54	0.020	0.3	6	126.4 ± 3.2	299.8 ± 20.2	0.3	
		Repeat	HR-IHE	K2003	127.0 ± 1.7	45	0.023	1.4	10	175.7 ± 1.7	126.8 ± 2.7	302.0 ± 20.1	0.9
			combined		127.1 ± 1.5	48	0.023	0.9	16				

^a K/Ca values are calculated as weighted means for the age spectra or using recombined totals of ³⁹Ar_K and ³⁷Ar_{Ca} for the total fusions. MSWD values for the age plateaus and inverse isochrons are calculated using N-1 and N-2 degrees of freedom, respectively. All samples from this study were monitored against FCT-3 biotite (28.04 Ma). Reported errors on the ⁴⁰Ar/³⁹Ar ages are on the 95% confidence level including 0.3–0.4% standard deviation in the J-value. We made difference between three types of ⁴⁰Ar/³⁹Ar analyses: [DGAS + TF], 1 or 2 degassing steps at 600–700°C followed by total fusion of the samples; [IHE], low-resolution incremental heating experiment with less than 10 heating steps; [HR-IHE], high-resolution incremental heating experiment with 15–30 heating steps. Data sources are as follows: [MSP1992], Pringle [1992]; [K2003], this study [2003].

brated to the primary K-Ar standard GA-1550 (98.79 ± 0.96 Ma, 1σ [Renne *et al.*, 1998]) using the explicit age equations after Karner and Renne [1998], Renne *et al.* [1998], and Min *et al.* [2000] as described by Koppers [2002]. An alternative recalibration to the FCT standard (28.48 ± 0.06 Ma, 1σ [Schmitz and Bowring, 2001]) based on single zircon U-Pb age dating is listed for comparison. This will bring the basement ages within the absolute reference frame for dating. To do so we have used the intercalibration ratios R for TCR to FCT (1.0112 ± 0.0010 , 1σ) and FCT to GA-1550 (0.27811 ± 0.00029 , 1σ) from Renne *et al.* [1998] and the corrected Steiger and Jäger [1977] decay constant of $5.530 \pm 0.097 \times 10^{-10}$ 1/yr (2σ) as reported by Min *et al.* [2000]. All constants used in the age calculations and their uncertainties are summarized in Table 2. Uncertainties are included for every input parameter in the $^{40}\text{Ar}/^{39}\text{Ar}$ age calculations, except for the $^{40}\text{Ar}/^{36}\text{Ar}$ and $^{38}\text{Ar}/^{36}\text{Ar}$ correction ratios in modern air, which generally are assumed invariable. Incremental heating plateau ages and argon-isotope isochron ages were calculated as weighted mean with $1/\sigma^2$ as weighting factor [Taylor, 1997] and as YORK2 least squares fit with correlated errors [York, 1969] using the ArArCALC v2.2 software [Koppers, 2002] (visit the ArArCALC Web site at <http://earthref.org/tools/ararcalc.htm>). These recalibrations have all been calculated using ArArCALC; this recalibration tool can also be downloaded as a separate Microsoft Excel program by following <http://earthref.org/cgi-bin/erda.cgi?n=139> to the EarthRef Digital Archive (ERDA). In this paper the errors on the $^{40}\text{Ar}/^{39}\text{Ar}$ ages are reported at the 95% confidence level, unless otherwise indicated.

3. Results and Discussion

[9] In this section, we start out by examining the $^{40}\text{Ar}/^{39}\text{Ar}$ age spectra (Figure 2) and discussing how to interpret these incremental heating experiments and how to judge the quality of the age results. Then we discuss our new age results for Sites 801C and 1149D in the context of the local basement configuration of the Pacific plate. We finish by discussing the implications for the nature

of Middle Jurassic fast spreading ridges in the Pacific and the Mesozoic timescale calibration.

3.1. The $^{40}\text{Ar}/^{39}\text{Ar}$ Geochronology of Low-K Basement Basalts

[10] Dating basaltic groundmass samples using $^{40}\text{Ar}/^{39}\text{Ar}$ incremental heating techniques has become a powerful tool when determining the age progressions for hot spot trails [Koppers *et al.*, 1998, 2003]. This is particularly true since crystalline groundmasses provide ages concordant with $^{40}\text{Ar}/^{39}\text{Ar}$ ages of co-magmatic minerals, allowing us to confidently interpret these groundmass ages as eruption ages [Koppers *et al.*, 2000]. In this study, we have been applying similar techniques to date basement samples for the Pacific crust as drilled during ODP Leg 185. Tholeiitic basement samples, however, have much lower potassium concentrations ($\text{K}/\text{Ca} < 0.005$) than seamount basalts and therefore are more vulnerable to disturbances by submarine alteration. Nevertheless, we observed similar argon release patterns characterized by (1) high apparent ages for the low-temperature steps, (2) well-resolved age plateaus at the intermediate temperature steps, and (3) discordant ages for the high-temperature steps. The low-temperature steps are further characterized by higher K/Ca ratios and atmospheric components than observed for the age plateau. These observations can be explained by the recoil of $^{39}\text{Ar}_K$ (increasing the apparent ages) in combination with the preferential degassing of alteration phases (increasing K/Ca ratios and the atmospheric component) that are located interstitially and on the surfaces of plagioclase/clinopyroxene in the groundmasses [Koppers *et al.*, 2000]. The intermediate temperature steps exhibit age plateaus that are high in their radiogenic component (80–100%) and have more constant K/Ca ratios. We conclude therefore that the effects of alteration and $^{39}\text{Ar}_K$ recoil to the plateau portions of the age spectra are negligible. This is confirmed by the fact that all plateau ages are consistent with their isochron ages (Figure 2; Table 1) at the 2σ confidence level and that $^{40}\text{Ar}/^{36}\text{Ar}$ intercept values are indistinguishable from the 295.5 atmospheric ratio, ruling out excess ^{40}Ar . These “internal” verifications are good indicators for the high quality of $^{40}\text{Ar}/^{39}\text{Ar}$

Table 2. Input Parameters for the ⁴⁰Ar/³⁹Ar Age Calculations

Parameter	Definition	Material	Value	Uncertainty Level	Source
<i>Age Calculation Parameters and Uncertainties</i>					
Decay Constants and Activities					
λ_{β^-}	Decay constant 40K -> 40Ca		$4.950 \pm 0.086 \times 10^{-10}$ 1/yr	2 σ	Beckinsale and Gale [1969]
λ_{40Ar}	Decay constant 40K -> 40Ar		$0.580 \pm 0.017 \times 10^{-10}$ 1/yr	2 σ	Beckinsale and Gale [1969]
λ_{tot}	Decay constant total 40K decay		$5.530 \pm 0.097 \times 10^{-10}$ 1/yr	2 σ	Beckinsale and Gale [1969]
A_{β^-}	Activity beta emission		28.27 ± 0.10 dps/g K	2 σ	Beckinsale and Gale [1969]
A_{40Ar}	Activity total 40Ar decay		3.31 ± 0.08 dps/g K	2 σ	Beckinsale and Gale [1969]
$\tau_{1/2}$	Half-life 40K		$1.253 \pm 0.022 \times 10^9$ yr	2 σ	Beckinsale and Gale [1969]
$\tau_{1/2}$	Half-life 39Ar		269 ± 3 yr	2 σ	Stoerner et al. [1965]
$\tau_{1/2}$	Half-life 37Ar		35.1 ± 0.1 days	2 σ	Stoerner et al. [1965]
$\tau_{1/2}$	Half-life 36Cl		3.1 days	2 σ	Weast [1981]
Physical Parameters					
W	Atomic weight of K		39.0983 ± 0.00012 g	2 σ	Garner et al. [1975]
⁴⁰ K/K	Abundance ratio 40K		$1.17 \pm 0.02 \times 10^{-4}$	2 σ	Audi et al. [1997]
N_0	Avogadro's number		$6.0221367 \pm 0.0000072 \times 10^{23}$	2 σ	Cohen and Taylor [1987]
S	Seconds in a tropical year		3.155693×10^7 s	2 σ	Min et al. [2000]
<i>Irradiation Constants and Uncertainties for the TRIGA-CLICIT Facility</i>					
40/36 Air	Isotopic ratio in modern air		295.5		Assumed constant
38/36 Air	Isotopic ratio in modern air		0.1869		Assumed constant
39/37 Ca	Calcium correction		0.000709 ± 0.000013	1 σ	Wijbrans et al. [1995]
38/37 Ca	Calcium correction		0.000032 ± 0.000007	1 σ	Wijbrans et al. [1995]
36/37 Ca	Calcium correction		0.000269 ± 0.000001	1 σ	Wijbrans et al. [1995]
40/39 K	Potassium correction		0.00165 ± 0.00041	1 σ	Wijbrans et al. [1995]
38/39 K	Potassium correction		0.01211 ± 0.00001	1 σ	Wijbrans et al. [1995]
K/Ca	Correction factor for molar K/Ca ratio		0.43		

Table 2. (continued)

Parameter	Definition	Material	Value	Uncertainty Level	Source
<i>K-Ar and $^{40}\text{Ar}/^{39}\text{Ar}$ Standards</i>					
Primary Standards					
GA-1550	McDougall Primary Standard	Biotite	97.90 ± 0.90 Ma 98.79 ± 0.96 Ma 98.5 ± 0.8 Ma	1σ 1σ 1σ	McDougall and Roksandic [1974] Renne et al. [1998] Spell and McDougall [2003]
Secondary Standards					
TCR	Taylor Creek Rhyolite	Sanidine	27.93 Ma 28.34 ± 0.28 Ma 28.04 ± 0.18 Ma	1σ 1σ 1σ	Duffield and Dalrymple [1990] Renne et al. [1998] Renne et al. [1998]
FCT	Fish Canyon Tuff	Sanidine	27.98 ± 0.08 Ma 28.48 ± 0.06 Ma 28.13 ± 0.24 Ma	1σ 1σ 1σ	Daze et al. [2003] Schmitz and Bowring [2001] Daze et al. [2003]
Intercalibration Ratios					
TCR ▲ FCT			1.01120 ± 0.00100	1σ	Renne et al. [1998]
FCT ▲ GA-1550			0.27811 ± 0.00029	1σ	Renne et al. [1998]

groundmass ages on these basement samples. The high-temperature steps are further characterized by a spike in the release of $^{37}\text{Ar}_{\text{Ca}}$ and strong decreases in the K/Ca ratios (Figure 2) that reflect the preferential outgassing of the calcium-rich phases, such as clinopyroxene and plagioclase. This spike in $^{37}\text{Ar}_{\text{Ca}}$ in all cases coincides with the onset of melt glazing as observed during the incremental heating experiments (see vertical lines in Figure 2) indicating that congruent partial melting has started. At the same point the age spectra may start to show discordant ages. For groundmasses with higher K/Ca ratios (such as ODP 1149D-10R-1 44-48 that has a K/Ca ratio of 0.023 typical of alkali basalts) the high-temperature ages may become lower due to recoil loss of irradiation-produced $^{37}\text{Ar}_{\text{Ca}}$ or redistribution of $^{39}\text{Ar}_{\text{K}}$ into the high-temperature phases, as is consistently observed for seamount basalts (Koppers et al., 2000). However, the basement tholeiites dated in this study with K/Ca < 0.005 show only minor deviations from the age plateaus (Figure 2). We believe that the increases in apparent age may be attributed to the fact that these samples are finer grained and have a lower modal amount of plagioclase and clinopyroxene in their groundmass, which makes the high-temperature phases vulnerable to the recoil of $^{39}\text{Ar}_{\text{K}}$ as well.

[11] Isotopic data from the incremental heating experiments display similarly predictable patterns in the $^{36}\text{Ar}/^{40}\text{Ar}$ vs. $^{39}\text{Ar}/^{40}\text{Ar}$ inverse isochron diagrams (see the right panels in Figure 2). In these diagrams, the discordant low-temperature (LT) steps start from the atmospheric intercept at 1/295.5 on the $^{36}\text{Ar}/^{40}\text{Ar}$ axis, followed by a curved approach toward the isochron, as indicated by the light blue arrows. These concave curves result from a combined decrease of the atmospheric component in the released argon gas (decreasing $^{36}\text{Ar}/^{40}\text{Ar}$) and the diminishing effects of the $^{39}\text{Ar}_{\text{K}}$ recoil (increasing $^{39}\text{Ar}/^{40}\text{Ar}$) during the incremental heating process [cf. Koppers et al., 2000]. In case the blue arrow crosses over the isochron line (see sample ODP 801C-15R-4 92-96) there is also a noticeable effect of radiogenic $^{40}\text{Ar}^*$ loss, increasing the $^{39}\text{Ar}/^{40}\text{Ar}$ ratios [cf. Kuiper, 2002] and lowering the apparent ages (see steps 3, 4 and 5

in the age plateau diagram). The discordant high-temperature (HT) steps also show a clear departure from the isochron, as indicated by the light orange arrows. These convex curves first move toward higher $^{39}\text{Ar}/^{40}\text{Ar}$ ratios and then quickly toward the atmospheric intercept for the final heating steps. It is noteworthy in this context that the “final melting points” fall on the reference line and very close to the atmospheric intercept on the $^{36}\text{Ar}/^{40}\text{Ar}$ axis. This indicates that the trapped argon in these groundmass samples have an initial $^{40}\text{Ar}/^{36}\text{Ar}$ ratio close to the 295.5 value.

[12] In these inverse isochron diagrams the data points representing the age plateaus form clear arrays that run parallel to the reference line between the plateau age on the $^{39}\text{Ar}/^{40}\text{Ar}$ axis and the atmospheric intercept on the $^{36}\text{Ar}/^{40}\text{Ar}$ axis (Figure 2). These arrays form distinct linear segments with a different angle when compared to the discordant LT and HT data curves, indicating that the age plateaus are not (significantly) affected by the same secondary processes and disturbances. In addition, each data array shows a good dispersion of its data points with high radiogenic contents. This makes the estimates of the isochron ages much better constrained than estimates of the $^{36}\text{Ar}/^{40}\text{Ar}$ intercepts (Table 1) [cf. *Kuiper*, 2002]. However, as discussed above, the location of the “final melting points” close to the atmospheric intercept strengthens our evidence for limited excess argon. Sample ODP 1149D-10R-1 44-48 shows these observations most clearly.

[13] On the basis of the above observations we conclude that groundmass $^{40}\text{Ar}/^{39}\text{Ar}$ dating can be used as a reliable dating technique in case no datable plagioclase phenocrysts are available, which is the case in the majority of the (tholeiitic) basement samples. Even when plagioclase phenocrysts are available for dating they are generally more depleted in potassium than the groundmasses, making $^{40}\text{Ar}/^{39}\text{Ar}$ age determinations increasingly more difficult. We attempted to date one plagioclase separate for sample ODP 801C-30R-4 37-41 resulting in a saddle-shaped age pattern with no useful age information, which are typical for very low-potassium feldspars ($\text{K}/\text{Ca} < 0.001$ [*McDougall and Harrison*, 1988]). However, by

careful preparation of the groundmass samples through (repeated) acid-leaching and hand-picking, we could avoid the inclusion of these discordant plagioclase pheno- and microcrysts in the groundmass samples and minimize the interfering effects of secondary mineral phases (such as clays, zeolites and carbonates) during $^{40}\text{Ar}/^{39}\text{Ar}$ experiments. Finally, by performing high-resolution incremental heating, which means more than 15 heating steps, we are able to furthermore decrease the effects of alteration and isolate enough of the primary argon signal to calculate meaningful age plateaus and isochrons.

3.2. Site 801C

[14] Three new basement samples were dated using high-resolution $^{40}\text{Ar}/^{39}\text{Ar}$ dating for Site 801C in the Pigafetta basin (Figure 1). This ODP Site was further deepened during Leg 185 penetrating tholeiitic basalt sequences that are typical for standard oceanic crust [*Plank et al.*, 2000; *Pockalny and Larson*, 2003]. We expanded the $^{40}\text{Ar}/^{39}\text{Ar}$ age database by dating one sample from the “upper pillow basalts” and two samples from the “lower massive flows” in the bottom section of this drill site (Figure 3). Sample ODP 801C-15R-4 92-96 was taken 614 mbsf and has a plateau age of 158.9 ± 3.3 Ma that is concordant with its 159.1 ± 5.5 Ma isochron age. This new age result is comparable to the 161.0 ± 5.4 Ma age of *Pringle* [1992] for sample ODP 801C-10R-5 53-58 that is positioned just above it, at 569 mbsf. *Pringle* [1992] also dated ODP 801C-10R-6 21-26 from the same position in the drill hole, but that sample resulted in a significantly older age of 174.1 ± 2.2 Ma in the light of our new data (Table 1). We argue here that this discordant age result of *Pringle* [1992] should be disregarded in the age compilation for Site 801C, because there was no acid-leaching applied to the basalt chips before analysis and because a limited four-step incremental heating schedule was applied during analysis. The basalt chips were degassed only at 600°C and 700°C followed by an intermediate temperature step at 1100°C and the total fusion step (for more details, see *Pringle* [1992]). The limited degassing of this submarine tholeiitic sample most likely did not remove all the LT and

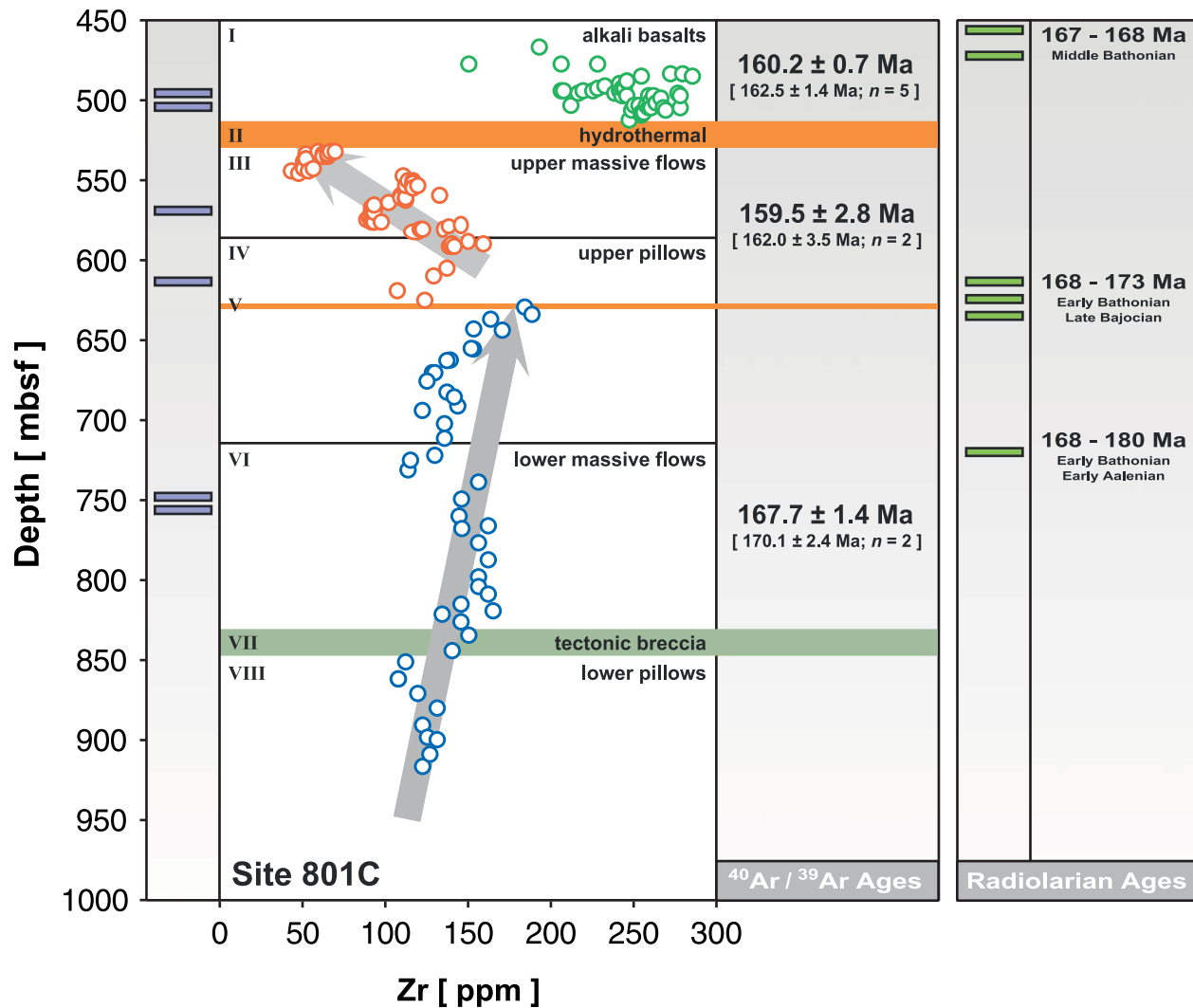


Figure 3. Downhole variation in Zr from shipboard XRF data at Site 801C [Plank et al., 2000] compared to available ⁴⁰Ar/³⁹Ar ages (see Tables 1 and 3). Three different magmatic sequences may be identified: (1) alkali basalts with enriched Zr relative to tholeiites, (2) upper tholeiites inter-layered between two hydrothermal layers showing an decreasing Zr trend up-section, and (3) lower tholeiites that show an increasing Zr trend up-section. Sequences (1) and (2) appear to be formed simultaneously around 160 Ma, while sequence (3) was formed ~7.3 Myr earlier around 167–168 Ma. Absolute age recalibrations with respect to the FCT standard as determined by zircon U-Pb dating (28.46 ± 0.06 Ma [Schmitz and Bowring, 2001]) are given within the square brackets. Specific sample positions for isotopic age dating are denoted in the left column. For comparison the radiolarian ages [Bartolini and Larson, 2001] determined for this ODP legacy basement site are given in the right-side column after recalibration to the Gradstein et al. [1995] timescale.

HT disturbances that we routinely observe (and resolve) for groundmass samples using high-resolution incremental heating schedules (Figure 2). This will leave a significant imprint of alteration on the ⁴⁰Ar/³⁹Ar age spectrum causing the 1100°C and fusion increments to yield older ages, which is typical for untreated submarine basaltic rocks [cf. McDougall and Harrison, 1988; Koppers et al.,

2000]. If we ignore sample ODP 801C-10R-5 53-58 we arrive at a combined age of 159.5 ± 2.8 Ma (n = 2) for the “upper massive flows and pillow basalts” of Sequences III and IV (Figure 3).

[15] Samples ODP 801C-30R-4 37-41 and 801C-31R-4 138-143 were taken well below the second hydrothermal layer in the deepest section of the

801C drill hole (Figure 3). For the second sample we repeated our argon analyses to yield a more precise estimate of its $^{40}\text{Ar}/^{39}\text{Ar}$ age. In our age compilation we therefore use the combined age of both incremental heating experiments resulting in an age of 166.7 ± 2.4 Ma that is comparable with the 168.2 ± 1.7 Ma age of the first sample (Table 1). The plateau ages for both samples are concordant at the 95% confidence level with their isochron ages and the $^{40}\text{Ar}/^{36}\text{Ar}$ estimates from the isochron analyses are similar to atmospheric air. This indicates that our $^{40}\text{Ar}/^{39}\text{Ar}$ age estimates are internally consistent and that their combined age of 167.7 ± 1.4 Ma ($n = 2$) represents the best $^{40}\text{Ar}/^{39}\text{Ar}$ age for the initial formation of this part of the Pacific oceanic crust during the Jurassic.

[16] On the basis of our new analyses, and combining with the previous results of *Pringle* [1992], we can now distinguish two age groups for Site 801C, as summarized in Figure 3. The 159.5 ± 2.8 Ma ($n = 2$) age for the “upper massive flows and pillow basalts” makes this tholeiitic series contemporaneous with the 160.2 ± 0.7 ($n = 5$) age for the overlying alkalic basalts in Sequence I [*Pringle*, 1992] (Figure 3). This results in an overall age of 160.1 ± 0.6 Ma ($n = 7$) for the entire “upper series” of Site 801C. However, the deepest drilled section of Site 801C has a decidedly older age of 167.7 ± 1.4 Ma ($n = 2$) and therefore appears to have formed 7.3 ± 1.5 Myr prior to the “upper series” basalts. On the basis of profound differences in the geochemistry of Site 801C (see the Zr compositions in Figure 3 [*Plank et al.*, 2000; *Fisk and Kelley*, 2002]) and variations in the dip of basalt flows down the hole [*Pockalny and Larson*, 2003], we can place this distinct age break at the second hydrothermal layer that is located 175 m deep into the Pigafetta basement. The basalts below this boundary layer comprise all the geochemical, lithological and morphological trends that represent standard oceanic crust created at fast spreading ridges, whereas the “upper series” basalts were created far off-axis [*Pockalny and Larson*, 2003], up to 7.3 Myr later (this study). As a consequence, the second hydrothermal layer marks the paleo-ocean floor subsequent to the

formation of this oceanic crust at the ridges. This scenario is supported by radiolarian assemblage data from six separate occurrences (Figure 3) [*Bartolini and Larson*, 2001] starting 258 m deep into the basement with Late Bajocian species (173 Ma) and ending at the top of this basement with Middle Bathonian species (167–168 Ma) as based on the geological timescale published by *Gradstein et al.* [1995]. Three of these occurrences (168–173 Ma; Early Bathonian and Late Bajocian species) coincide with the second hydrothermal layer and show that the oldest sediments were deposited immediately after the production of the juvenile oceanic crust. In this context, the “upper series” basalts most likely were formed by multiple sill intrusions in the sediment pile on top of this paleo-ocean floor. Since the basal sediments at Site 801C are slightly (but significantly) older at 167–168 Ma, we have to conclude that the 160.1 ± 0.6 Ma basalts must have intruded as sills close to the base of the accumulated sediments, while forming the ~ 20 m thick hydrothermal layer of Sequence II [*Alt et al.*, 1992; *Pockalny and Larson*, 2003]. This scenario is supported by the presence of iron-stained and tilted sediments (up to 60° dip) directly above the alkalic unit [*Lancelot et al.*, 1990; *Pockalny and Larson*, 2003].

[17] The new 167.7 ± 1.4 Ma age for the initial formation of the Pigafetta basement at Site 801C allows us to better define the half-spreading rate for the Pacific plate during this time interval. We will follow the same calculation method as *Pockalny and Larson* [2003] by comparing the 167.7 Ma age to the age of magnetic anomaly M25 (154.0 ± 3.2 Ma [*Gradstein et al.*, 1995]) that is located ~ 900 km toward the Northwest. We arrive at half-spreading rate ranging between 49–99 km/Myr (with an average of 66 km/Myr) that indicates intermediate to ultrafast spreading. At this half-spreading rate, the sills of the “upper series” would have been produced 400–600 km off-axis from its Jurassic spreading center.

3.3. Site 1149D

[18] Only one sample was dated using high-resolution $^{40}\text{Ar}/^{39}\text{Ar}$ dating for Site 1149D (ODP Leg 185; Figure 1). This Site is located on the Pacific

plate close to the Mariana Trench and was drilled in magnetic lineation M12 in the Nadezhda basin, predicting an age of 134.2 ± 2.1 Ma on the basis of the *Channell et al.* [1995] or *Gradstein et al.* [1995] timescales. The M12 designation is based on the distinctive $\delta^{13}\text{C}$ isotopic shift that was discovered at drill site 1149B and that is characteristic of the Valanginian Oceanic Anoxic Event (correlated to M11) in land sections [*Bartolini, 2003*]. This isotopic anomaly and the 50 m of sediments beneath it, requires the (real) basement to correlate with M12r [*Bartolini, 2003*]. Sample ODP 1149D-10R-1 44-48 (350 mbsf) was dated twice to improve on the precision of the $^{40}\text{Ar}/^{39}\text{Ar}$ age determinations. The combined $^{40}\text{Ar}/^{39}\text{Ar}$ plateau age is 127.1 ± 1.5 Ma and is concordant with the 126.8 ± 2.7 Ma isochron age on the 95% confidence level (Table 1; Figure 2). Even though only 48% of the released $^{39}\text{Ar}_k$ gas is used in the calculations, the above mentioned age concordance illustrates the high-quality of the age determinations. However, the 127.1 ± 1.5 Ma age is significantly younger than expected on the basis of the *Gradstein et al.* [1995] age for the M12 magnetic anomaly and the Valanginian nanofossils (132 Ma) found in the basal sediments (species *T. verenae* in Site 1149B [*Plank et al., 2000*]). Calcareous nanofossil data show an age range between Late Valanginian and Hauterivian age (Figure 3) [*Lozar and Tremolada, 2003*], again indicating that this basement may be older than the 127.1 Ma isotopic age. Even when including all systematic errors in the $^{40}\text{Ar}/^{39}\text{Ar}$ age calculations, we arrive at an absolute age estimate that is still significantly younger at 127.0 ± 3.6 Ma (Table 3). As with Site 801C, this may point to sills above the Pacific basement, although hydrothermal layers are missing in the 1149D drill hole and this drilled crust comprises standard pillow basalt sequences for fast spreading oceanic crust (note though that the dated sample has K/Ca ratios typical of alkali basalts; compare data in Table 1). These possible sills at Site 1149D may be part of the Early Cretaceous intraplate events that have produced dolerite intrusions in the Pacific crust at Site 800 and 802 around 114–126 Myr ago (Figure 1). The implications of this age discrepancy with

respect to the calibration of the timescale will be discussed in detail below.

3.4. Nature of Middle Jurassic Fast Spreading Ridges

[19] The Jurassic oceanic crust encountered at Site 801C in the Pigafetta basin is characterized by basalt sequences that arguably formed off-axis by episodic intrusions into sediments, perhaps associated with the formation of small near-ridge seamounts [*Castillo et al., 1992; Zindler et al., 1984*]. A clear contribution of ocean island basalt (OIB) mantle sources in the isotope geochemistry of the Site 801C basalts suggests that the Pigafetta basement was produced from a mixture of depleted MORB mantle and enriched OIB mantle sources [*Castillo et al., 1992*]. In alternative models, the off-axis basalt sequences can be explained by “fluctuating ridge magmatism” causing the collapse of the oceanic basement following a period of enhanced volcanism [*Pockalny and Larson, 2003*] that is typical for fast spreading ridges. These collapses will fracture the oceanic crust off-axis and allow magma transport into the upper parts of the Pacific basement, causing the later intrusions. The presence of a 10 m thick tectonic breccia on top of Sequence VII (Figure 3) may be related to this fracturing [*Pockalny and Larson, 2003*].

[20] In this model, the sills most likely would have been produced in isolated parts of the Pacific plate, but on the scale of the entire Pacific plate they may represent significant volumes of more enriched basaltic volcanism with typical OIB or E-MORB geochemical signatures. At Site 801C the top 175 m of the basaltic basement was formed off-axis, whereas various sills were encountered at the 800, 802 and 1149 basement sites (Figure 1) [*Pringle, 1992; Castillo et al., 1992; this study*]. This indicates that sill intrusions should be considered a common mode of volcanism in the construction of oceanic plates. In consequence, the presence of sills in the West Pacific oceanic crust needs to be considered when modeling geochemical mass balances at subduction zones, in particular, since these more “enriched” basaltic components are also more fertile and might be preferentially sampled during partial melting in these subduction zones

Table 3. Recalibration of the $^{40}\text{Ar}/^{39}\text{Ar}$ Ar Age Estimates Toward Absolute Ages^a

Sample Type	Study Identifier	Internal Age		Absolute Age		Error Contributions				Absolute Age	
		Age $\pm 2\sigma$, Ma TCR or FCT	Age $\pm 2\sigma$, Ma	Age $\pm 2\sigma$, Ma GA-1550	40K/K, %	IIR, %	40Ar(ϵ), %	40Ar(β), %	40Ar*(p), %	K(p), %	Age $\pm 2\sigma$, Ma, FCT U-Pb
<i>Pigafetta Basin (Sites 801B and 801C), 18°38.538'N, 156°21.588'E</i>											
Alkalic Basalts											
801C-01R-1 109-119	MSP1992	157.8 \pm 0.7	159.9 \pm 2.0	159.9 \pm 2.0	0.1	14.5	70.4	0.0	13.0	2.1	162.5 \pm 1.4
	MSP1992	157.6 \pm 1.6	159.9 \pm 4.4	159.9 \pm 4.4	0.1	14.7	70.3	0.0	12.9	2.1	162.4 \pm 3.1
	MSP1992	156.2 \pm 1.6	158.4 \pm 4.4	158.4 \pm 4.4	0.1	16.8	68.5	0.0	12.6	2.1	161.0 \pm 3.1
	MSP1992	161.5 \pm 1.8	163.8 \pm 4.6	163.8 \pm 4.6	0.1	6.8	76.7	0.0	14.1	2.3	166.4 \pm 3.3
801B-44R-3 13-22	MSP1992	158.1 \pm 1.0	160.4 \pm 4.3	160.4 \pm 4.3	0.1	21.0	65.1	0.0	12.0	1.9	162.9 \pm 2.8
	MSP1992	155.0 \pm 2.0	157.2 \pm 4.5	157.2 \pm 4.5	0.1	64.0	29.7	0.0	5.5	0.9	159.7 \pm 3.3
Tholeiites: Upper Massive Flows and Pillow Basalts											
801C-10R-5 53-58	MSP1992	158.6 \pm 5.4	160.9 \pm 6.9	160.9 \pm 6.9	0.0	39.7	49.6	0.0	9.1	1.5	162.0 \pm 3.5
801C-15R-4 92-96	K2002	158.9 \pm 3.3	158.8 \pm 5.2	158.8 \pm 5.2	0.1	13.6	71.2	0.0	13.1	2.1	163.4 \pm 6.2
Tholeiites: Lower Massive Flows											
801C-30R-4 37-41	K2002	167.7 \pm 1.4	167.4 \pm 3.4	167.4 \pm 3.4	0.1	17.8	67.7	0.0	11.5	1.9	170.1 \pm 2.4
801C-31R-4 138-143	K2002	168.2 \pm 1.7	168.1 \pm 4.6	168.1 \pm 4.6	0.1	127.0 \pm 3.6	62.5	0.0	12.5	2.0	170.8 \pm 3.2
	K2002	166.7 \pm 2.4	166.6 \pm 4.9	166.6 \pm 4.9	0.1	17.8	67.7	0.0	12.5	2.0	169.2 \pm 3.6
Basaltic Basement											
1149D-10R-1 44-48	K2002	127.1 \pm 1.5	127.0 \pm 3.6	127.0 \pm 3.6	0.1	127.0 \pm 3.6	67.7	0.0	12.5	2.0	129.0 \pm 2.6

Mariana Trench (Site 1149D), 31°18.790' N, 143°24.030' E

^aThe column with internal ages is displayed for comparison because it forms the starting point in the recalibration. Note that MSP1992 used TCR = 27.92 Ma to calculate its internal $^{40}\text{Ar}/^{39}\text{Ar}$ ages; K2003 used FCT = 28.04 Ma for these calculations. The absolute ages have been calculated using the explicit age equations of *Min et al.* [2000] as detailed by *Koppers* [2002] and using the input parameters as listed in Table 2. Two recalibrations have been performed: (1) recalibration toward the primary K-Ar standard GA-1550 (98.79 \pm 0.96 Ma [Renne *et al.*, 1998]) and (2) recalibration toward the FCT age standard as calibrated with single zircon U-Pb dating (28.48 \pm 0.06 Ma [Schmitz and Bowring, 2001]). The contribution (in%) for each type of systematic error is indicated for the GA-1550 recalibration only, showing that the most important contributors are the errors in the intercalibration factor (R), the uncertainty in the value for the $^{40}\text{Ar}_e$ decay activity constant and the uncertainty in the determination of the composition of the primary standard ($^{40}\text{Ar}^*$ and K). We made difference between three types of $^{40}\text{Ar}/^{39}\text{Ar}$ analyses: [DGAS + TF], 1 or 2 degassing steps at 600–700°C followed by total fusion of the samples; [IHE], low-resolution incremental heating experiment with less than 10 heating steps; [HR-IHE], high-resolution incremental heating experiment with 15–30 heating steps. Data sources are as follows: [MSP1992], *Pringle* [1992]; [K2003], this study (2003).

[cf. *Phipps Morgan and Morgan, 1999; Phipps Morgan, 2001*].

3.5. Mesozoic Timescale Calibration

[21] In this study, we were able to assign an improved age of 167.7 ± 1.4 Ma to the Pigafetta basin at Site 801C, which represents the best age estimate to this day for the initial formation of the Pacific plate. This new age estimate also forms an important calibration point on the Geological Reversal Timescale (GRTS) since it represents the old end of the so-called M-series or Mesozoic magnetic anomalies [*Cande and Kent, 1992*]. Site 1149D gives another important calibration point in these M-series at anomaly M12, although its 127.1 ± 1.5 Ma age appears to be younger than expected from current timescale compilations (~ 134 Ma). We note here that the 167.7 and 127.1 Ma ages are not absolute isotopic age determinations; they are typical internal $^{40}\text{Ar}/^{39}\text{Ar}$ ages that have been calculated relative to the FCT dating standard with an age of 28.04 Ma [*Renne et al., 1994*] and include analytical and J-value errors only. These internal $^{40}\text{Ar}/^{39}\text{Ar}$ ages therefore can be compared only to other $^{40}\text{Ar}/^{39}\text{Ar}$ ages that have been calibrated against the same standard with the exact same age value. To make our ages applicable and useful for timescale calibrations, we need to recalibrate all our ages to a primary K-Ar dating standard and incorporate each source of systematic and analytical error [*Renne et al., 1998; Min et al., 2000; Koppers, 2002*]. Only then can we place our new age estimates within an “absolute” framework for geological age determinations and with confidence compare these $^{40}\text{Ar}/^{39}\text{Ar}$ ages with other age estimates, such as derived by U-Pb mineral dating.

[22] We have recalibrated all ages from Sites 801C and 1149D to the GA-1550 primary K-Ar dating standard that first was introduced by McDougall and Roksandic in 1974, but which recently was re-analyzed by *Renne et al.* [1998], resulting in an age of 98.79 ± 0.96 Ma, and *Spell and McDougall* [2003], resulting in a similar age of 98.5 ± 0.8 Ma. We also performed the recalibration using the secondary FCT standard as independently calibrated using single zircon U-Pb dating (28.48 ± 0.06 Ma

[*Schmitz and Bowring, 2001*]). In our recalibrations we have included all sources of error as listed in Table 2 and we display the results in Table 3. It should be noted here that the actual ages as originally measured against the FCT-3 biotite standard (this study) do not vary that much in this recalibration (only ~ 0.1 Myr) but that the ages of *Pringle* [1992] show a significant increase of ~ 2.4 Myr. This is mostly caused by the fact that *Pringle* [1992] used an old calibration value for the TCR dating standard at 27.92 Ma that now has been re-determined at 28.34 ± 0.28 Ma using modern dating techniques (Table 2). More importantly, the error estimates for all our age data have increased significantly: by 250%. This dramatic increase in the uncertainties can be entirely attributed to the introduction of systematic errors for the $^{40}\text{K} \rightarrow ^{40}\text{Ar}$ decay constants, $^{40}\text{K}/\text{K}$ abundance ratio and standard inter-calibrations (Table 3). However, these increased uncertainties are now more realistic and, in the context of the calibration of the GRTS, allows for comparison with other dating techniques. We arrive at absolute ages of 167.4 ± 3.4 Ma and 127.0 ± 3.6 Ma for Site 801C and 1149D, respectively. Recalibration using FCT as determined by U-Pb methods results in ~ 2.5 Myr older ages at 170.1 ± 2.4 Ma and 129.0 ± 2.6 Ma, which reflects the current $\sim 1.5\%$ inconsistency existing between the $^{40}\text{Ar}/^{39}\text{Ar}$ and U-Pb isotopic dating systems [*Schmitz and Bowring, 2001; Renne et al., 2003*].

[23] The 167.4 ± 3.4 Ma age for Site 801C is similar to the estimate by *Kent and Gradstein* [1985] for this site at 169 Ma and it is concordant (within the 95% confidence limit) with the *Harland et al.* [1990] timescale estimate at 161.3 ± 5 Ma. It also overlaps with the *Gradstein et al.* [1995] timescale (GRAD95) that is based on high-temperature $^{40}\text{Ar}/^{39}\text{Ar}$ incremental heating ages exclusively (see Figure 4). However, the $^{40}\text{Ar}/^{39}\text{Ar}$ ages used in the GRAD95 timescale were all recalibrated toward the MMhb-1 age standard at 520.4 Ma. Recalibration to the $^{40}\text{Ar}/^{39}\text{Ar}$ standard GA-1550 will cause the GRAD95 timescale to shift approximately 1 Myr toward older ages, whereas recalibration toward the U-Pb FCT age standard will increase this shift another ~ 2.5 Myr. In either case,

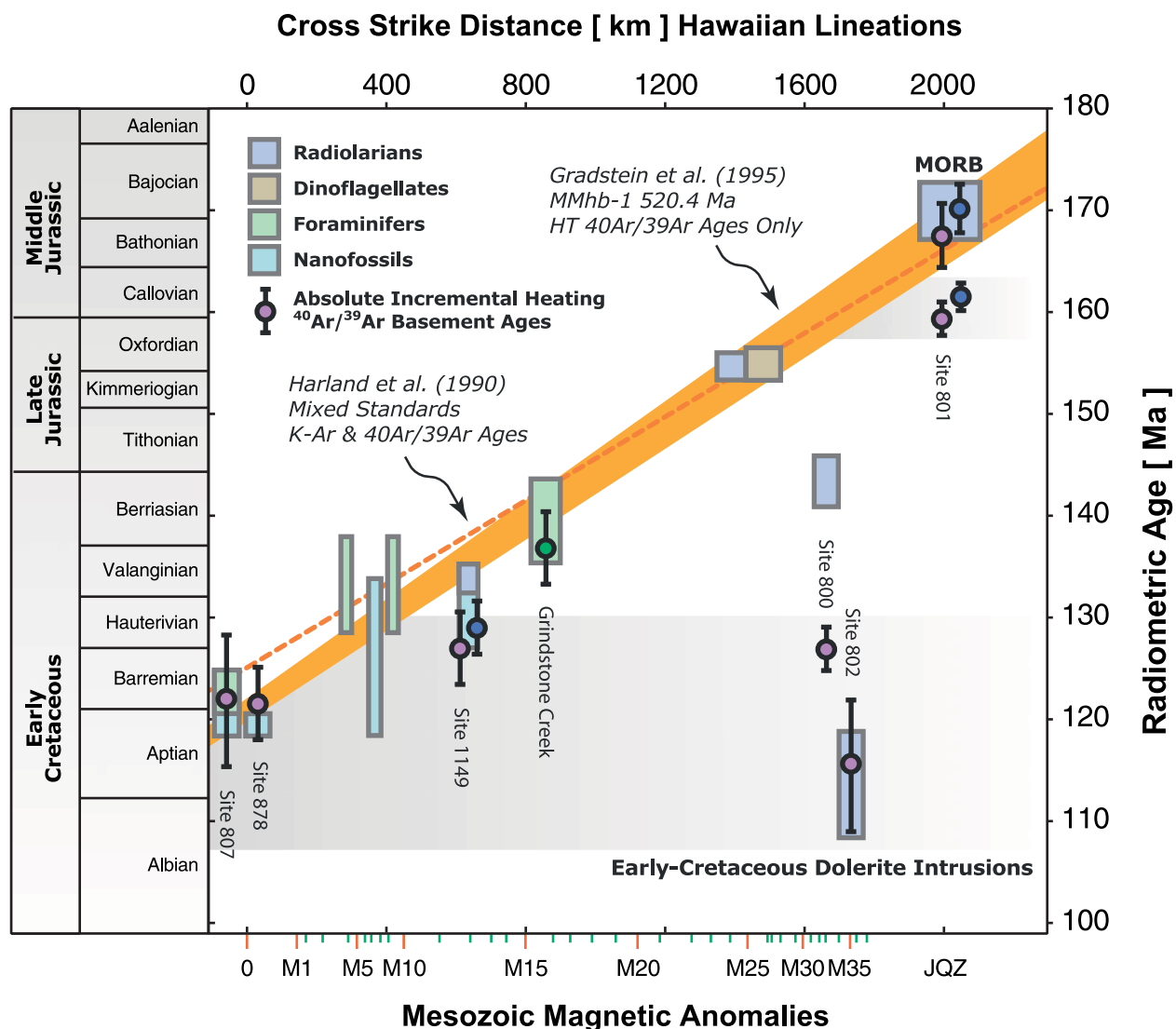


Figure 4. Mesozoic time calibration after Pringle [1992]. The ⁴⁰Ar/³⁹Ar ages from this study are compared to the Harland et al. [1990] and Gradstein et al. [1995] timescale. The displayed ages are recalibrated to the primary GA-1550 K-Ar age standard (98.79 ± 0.96 Ma; filled pink circles) and the FCT standard as determined by zircon U-Pb dating (28.46 ± 0.06 Ma; filled blue circles). We also show the calibration points for Site 807 and 878 that calibrate the M0 polarity chron [Mahoney et al., 1993; Koppers, 1998; Pringle et al., 2003] and for the Grindstone Creek in California that calibrates the M16 chron [Bralower et al., 1990] using U-Pb zircon dating (filled green circle). These calibration points have been recalibrated to GA-1550 and their uncertainties reflect absolute errors. All errors are on the 2σ level and reflect absolute age uncertainties.

the absolute 167.4 ± 3.4 Ma (GA-1550) or 171.1 ± 2.4 Ma (U-Pb FCT) ages for Site 801C are consistent with the GRAD95 timescale. Note that all these timescales assumes a constant spreading rate for the Pacific during the entire Jurassic and Cretaceous, which is an oversimplification dictated by the few tie points that have been calibrated by isotopic dating.

[24] The story for Site 1149D is more complicated since the new ⁴⁰Ar/³⁹Ar age of 127.0 ± 3.6 Ma (GA-1550) or 129.0 ± 2.6 Ma (U-Pb FCT) is significantly younger than the M12 age in the GRAD95 timescale (Figure 4). This difference remains even after recalibration of the GRAD95 timescale (see above). In the light of these observations we may consider two explanations. In the

Table A1. High-Resolution Incremental Heating Experiment Information

Sample Number	Sample Type	Archive Name	ERDA Hyperlink
ODP 801C-15R-4 92-96	Groundmass	00C2252.zip	http://earthref.org/cgi-bin/erda.cgi?n=140
ODP 801C-30R-4 37-41	Groundmass	00C2272.zip	http://earthref.org/cgi-bin/erda.cgi?n=141
ODP 801C-30R-4 37-41	Plagioclase	00C1973.zip	http://earthref.org/cgi-bin/erda.cgi?n=142
ODP 801C-31R-4 138-143	Groundmass	00C1937.00C2193.zip	http://earthref.org/cgi-bin/erda.cgi?n=143
ODP 1149D-10R-1 44-48	Groundmass	00C1957.00C2215.zip	http://earthref.org/cgi-bin/erda.cgi?n=144

first explanation, sample ODP 1149D-10R-1 44-48 is typical N-MORB and represents normal oceanic crust, which seems to be the case for the entire section of pillow basalts drilled at Site 1149D [Plank *et al.*, 2000]. If this is correct, it means that our new $^{40}\text{Ar}/^{39}\text{Ar}$ age represents the formation of the Pacific oceanic crust during the Early Cretaceous and therefore this age should be considered in an improved version of the GRTS. However, as a direct result, inclusion of this calibration point in the GRTS would make the age boundaries between 3 and 6 Myr younger for the Early Cretaceous stages. This revision would be consistent with the calibration of M16 at the Grindstone Creek in California (137.1 ± 3.2 Ma [Bralower *et al.*, 1990]), but it will make the 1149D age inconsistent with the key calibrations of M0r for Site 878 at MIT Guyot (121.8 ± 3.8 Ma [Koppers, 1998; Pringle *et al.*, 2003]) and Site 807 at the Ontong Java Plateau (122.3 ± 7.8 Ma [Mahoney *et al.*, 1993]). In the second explanation, sample ODP 1149D-10R-1 44-48 is an enriched E-MORB basalt that is (somehow) related to a massive unit encountered in the bottom 30 m of the 1149D drill hole [Plank *et al.*, 2000]. The relatively high K/Ca ratio for the dated sample (Table 1) actually may agree with such an alkali rich source, maybe representing another intrusive event up to 6 Myr younger than the underlying Pacific crust formed at the mid-oceanic ridges, in an analogous scenario as described for Site 801C. At this stage, we cannot easily decide between these explanations, because we lack important geochemical and structural data to support either of these two explanations, and because we are limited to only one $^{40}\text{Ar}/^{39}\text{Ar}$ age. This makes the interpretation for Site 1149D inconclusive, and would require deepening of the drill hole in the future and further high-resolution $^{40}\text{Ar}/^{39}\text{Ar}$ dating to solve this geological puzzle.

One important outcome of such an exercise would be to determine the importance of sill intrusions in the formation of the oceanic crust, as we have been describing in detail for Site 801C.

4. Summary

[25] In this paper we have reported new $^{40}\text{Ar}/^{39}\text{Ar}$ ages for the oldest Pacific oceanic floor at ODP Site 801C in the Pigafetta basin and Site 1149D close to the Izu-Bonin subduction zone in the Nadezhda basin. The oldest part of the Pacific plate was formed at the spreading ridges around $167.4 \pm 1.4/3.4$ Ma ($n = 2$, 2σ internal/absolute error) offering a most important calibration point on the Geological Reversal Timescale (GRTS). This mid-ocean ridge basalt sequence, however, is overlain by tholeiites and alkali basalts that were formed 7.3 ± 1.5 Myr later, around 160.1 ± 0.6 Ma ($n = 7$, 2σ internal error). The older age group is confirmed independently by radiolarian ages and by profound differences in the structural and chemical characteristics of this basement section. This indicates that substantial volcanic and hydrothermal activity took place 400–600 km away from the spreading ridges, on the basis of a Jurassic ~ 66 km/Myr half spreading rate in the Pacific. Site 1149D gives another important calibration point on the GRTS around $127.0 \pm 1.5/3.6$ Ma ($n = 1$, 2σ internal/absolute error) for the M12 anomaly, but this age is slightly younger when compared to current timescale compilations (134 ± 2.1 Ma [Gradstein *et al.*, 1995]). Recalibration using current age standards and inclusion of all systematic errors in the age calculation cannot explain this discrepancy. This might suggest that the dated basalt from Site 1149D is not formed at a spreading center, but rather that it is part of the Early Cretaceous intraplate events that have produced

dolerite sills in the Pacific crust at Site 800 and 802 around 114–126 Myr ago. Our observations indicate that off-axis intrusions or volcanism should be considered a common mode of volcanism in the construction of oceanic plates.

Appendix A: The $^{40}\text{Ar}/^{39}\text{Ar}$ Analytical Data

[26] All new $^{40}\text{Ar}/^{39}\text{Ar}$ age data reported in this study have been calculated using ArArCALC v2.2 (A. Koppers, 2002; <http://earthref.org/tools/ararcalc.htm>), and their resulting *.AGE files have been included in this electronic appendix. The same files also have been saved in the standard Microsoft Excel format (with the *.XLS extension) and can be opened without running ArArCALC. In Table A1 each high-resolution incremental heating experiment is listed together with their filenames and a URL to download these files from the EarthRef Digital Archive (ERDA).

[27] Note that all electronic data supplements that are related to this publication can be listed online EarthRef by selecting the <http://earthref.org/cgi-bin/err.cgi?n=1444> link and by following the Quick Links. Follow <http://earthref.org/cgi-bin/erda.cgi?p=13> to retrieve all the available contributions to the Subduction Factory theme in G-cubed.org.

[28] The ArArCALC v2.2 software can be directly downloaded using the <http://earthref.org/cgi-bin/erda.cgi?n=133> link, whereas the ArArCALIBRATIONS tool can be retrieved from <http://earthref.org/cgi-bin/erda.cgi?n=139>.

Acknowledgments

[29] We thank John Huard and Lew Hogan for their technical support in the OSU argon dating laboratory. Financial support is by JOI-USSAC #F001128. We also thank an anonymous reviewer, Anachiara Bartolini and John Ludden for their thoughtful reviews.

References

Abrams, L. J., R. L. Larson, T. H. Shipley, and Y. Lancelot, Cretaceous volcanic sequences and Jurassic oceanic crust in the east Mariana and Pigafetta basins of the western Pacific, in *The Mesozoic Pacific: Geology, Tectonics, and Volcanism*,

- Geophys. Monogr. Ser.*, vol. 77, edited by M. S. Pringle et al., pp. 77–101, Washington, D. C., 1993.
- Alt, J. C., C. France-Lanord, P. A. Floyd, P. Castillo, and A. Galy, Low-temperature hydrothermal alteration of Jurassic ocean crust, Site 801, *Proc. Ocean Drill. Program Sci. Results*, 129, 415–427, 1992.
- Audi, G., O. Bersillon, J. Blachot, and A. H. Wapstra, The NUBASE evaluation of nuclear and decay properties, *Nucl. Phys. A*, 264, 1–124, 1997.
- Bartolini, A., Cretaceous radiolarian biochronology and carbon isotope stratigraphy of ODP Site 1149 (Northwestern Pacific, Nadezhda basin), *Proc. Ocean Drill. Program Sci. Results*, 185, 1–17, 2003.
- Bartolini, A., and R. L. Larson, Pacific microplate and the Pangea supercontinent in the Early to Middle Jurassic, *Geology*, 29, 735–738, 2001.
- Beckinsale, R. D., and N. H. Gale, A reappraisal of the decay constants and branching ratio of ^{40}K , *Earth Planet. Sci. Lett.*, 6, 289–294, 1969.
- Bralower, T. J., K. R. Ludwig, J. D. Obradovich, and D. L. Jones, Berriasian (Early Cretaceous) radiometric ages from the Grindstone-Creek Section, Sacramento Valley, California, *Earth Planet. Sci. Lett.*, 98(1), 62–73, 1990.
- Cande, S. C., and D. V. Kent, A new geological reversal time scale for the Late Cretaceous and Cenozoic, *J. Geophys. Res.*, 97, 13,917–13,951, 1992.
- Castillo, P. R., P. A. Floyd, and C. France-Lanord, Isotope geochemistry of Leg 129 basalts: Implications for the origin of the widespread Cretaceous volcanic event in the Pacific, *Proc. Ocean Drill. Program Sci. Results*, 129, 405–513, 1992.
- Channell, J. E. T., E. Erba, M. Nakanishi, and K. Tamaki, Late Jurassic-Early Cretaceous time scales and oceanic magnetic anomaly block models, in *Geochronology Time Scales and Global Stratigraphic Correlation*, edited by W. A. Berggren et al., *Spec. Publ. Soc. Econ. Paleontol. Mineral.*, 54, 51–63, 1995.
- Cohen, E. R., and B. N. Taylor, The 1986 CODATA recommended values of the fundamental physical constants, *J. Res. Natl. Bur. Stand. U.S.*, 92, 85–95, 1987.
- Daze, A., J. K. W. Lee, and M. Villeneuve, An intercalibration study of the Fish Canyon sanidine and biotite Ar-40/Ar-39 standards and some comments on the age of the Fish Canyon Tuff, *Chem. Geol.*, 199(1–2), 111–127, 2003.
- Duffield, W. A., and G. B. Dalrymple, The Taylor Creek rhyolite of New Mexico: A rapidly emplaced field of domes and flows, *Bull. Volcanol.*, 52, 475–478, 1990.
- Fisk, M., and K. A. Kelley, Probing the Pacific's oldest MORB glass: Mantle chemistry and melting conditions during the birth of the Pacific plate, *Earth Planet. Sci. Lett.*, 202, 741–752, 2002.
- Garner, E. L., T. J. Murphy, J. W. Gramlich, P. J. Paulsen, and I. L. Barnes, Absolute isotopic abundance ratios and the atomic weight of a reference sample of potassium, *J. Res. Natl. Bur. Stand., Sect. A*, 79, 713–725, 1975.
- Gradstein, F. M., F. P. Agterberg, J. G. Ogg, J. Hardenbol, P. Van Veen, J. Thierry, and Z. Huang, A Triassic, Jurassic and Cretaceous time scale, in *Geochronology Time Scales*

- and *Global Stratigraphic Correlation*, edited by W. A. Berggren et al., *Spec. Publ. Soc. Econ. Paleontol. Mineral.*, 54, 95–126, 1995.
- Harland, W. B., R. L. Armstrong, A. V. Cox, L. E. Craig, A. G. Smith, and D. G. Smith, *A Geologic Time Scale*, 265 pp., Cambridge Univ. Press, New York, 1990.
- Hurst, S. D., J. A. Karson, and K. L. Verosub, Paleomagnetism of tilted dikes in fast spread oceanic crust exposed in the Hess Deep rift: Implications for spreading and rift propagation, *Tectonics*, 13, 789–802, 1994.
- Karner, D. B., and P. R. Renne, $^{40}\text{Ar}/^{39}\text{Ar}$ geochronology of Roman volcanic province tephra in the Tiber river valley: Age calibration of middle Pleistocene sea-level changes, *Geol. Soc. Am. Bull.*, 110, 740–747, 1998.
- Karson, J. A., E. M. Klein, S. D. Hurst, C. E. Lee, P. A. Rivizzigno, D. Curewitz, A. R. Morris, and Hess Deep '99 Scientific Party, Structure of uppermost fast-spread oceanic crust exposed at the Hess Deep Rift: Implications for sub-axial processes at the East Pacific Rise, *Geochem. Geophys. Geosyst.*, 3, doi:10.1029/2003GC000574, 2002.
- Kent, D. V., and F. M. Gradstein, A Cretaceous and Jurassic chronology, *Geol. Soc. Am. Bull.*, 96, 1419–1427, 1985.
- Koppers, A. A. P., $^{40}\text{Ar}/^{39}\text{Ar}$ geochronology and isotope geochemistry of the West Pacific seamount province: Implications for absolute Pacific plate motions and the motion of hotspots, Ph.D., 263 pp., Vrije Univ. eit Amsterdam, Amsterdam, Netherlands, 1998.
- Koppers, A. A. P., ArArCALC—Software for $^{40}\text{Ar}/^{39}\text{Ar}$ age calculations, *Comput. Geosci.*, 28, 605–619, 2002. (Available at <http://earthref.org/tools/ararcalc.htm>.)
- Koppers, A. A. P., H. Staudigel, J. R. Wijbrans, and M. S. Pringle, The Magellan seamount trail: Implications for Cretaceous hotspot volcanism and absolute Pacific plate motion, *Earth Planet. Sci. Lett.*, 163, 53–68, 1998.
- Koppers, A. A. P., H. Staudigel, and J. R. Wijbrans, Dating crystalline groundmass separates of altered Cretaceous seamount basalts by the $^{40}\text{Ar}/^{39}\text{Ar}$ incremental heating technique, *Chem. Geol.*, 166, 139–158, 2000.
- Koppers, A., H. Staudigel, J. R. Wijbrans, and M. Pringle, Short-lived and discontinuous intraplate volcanism in the South Pacific: Hot spots or extensional volcanism?, *Geochem. Geophys. Geosyst.*, 4, doi:10.1029/2003GC000533, in press, 2003.
- Kuiper, Y. D., The interpretation of inverse isochron diagrams in $^{40}\text{Ar}/^{39}\text{Ar}$ geochronology, *Earth Planet. Sci. Lett.*, 203, 499–506, 2002.
- Lancelot, Y., et al., *Proceedings of the Ocean Drilling Program, Initial Reports*, vol. 129, Ocean Drill. Program, College Station, Tex., 1990.
- Lozar, F., and F. Tremolada, Calcareous nannofossil biostratigraphy of Cretaceous sediments recovered at ODP Site 1149 (Leg 185, Nadezhda Basin, Western Pacific), *Proc. Ocean Drill. Program Sci. Results*, 185, 1–21, 2003.
- Mahoney, J. J., M. Storey, R. A. Duncan, K. J. Spencer, and M. S. Pringle, Geochemistry and geochronology of leg 130 basement lavas: Nature and origin of the Ontong Java Plateau, *Proc. Ocean Drill. Program Sci. Results*, 130, 3–22, 1993.
- McDougall, I., and T. M. Harrison, *Geochronology and Thermochronology by the $^{40}\text{Ar}/^{39}\text{Ar}$ Method*, 212 pp., Oxford Univ. Press, New York, 1988.
- McDougall, I., and Z. Roksandic, Total fusion $^{40}\text{Ar}/^{39}\text{Ar}$ ages using HIFAR reactor, *J. Geol. Soc. Aust.*, 21, 81–89, 1974.
- Min, K., R. Mundil, P. R. Renne, and K. R. Ludwig, A test for systematic errors in $^{40}\text{Ar}/^{39}\text{Ar}$ geochronology through comparison with U/Pb analysis of a 1.1-Ga rhyolite, *Geochim. Cosmochim. Acta*, 64, 73–98, 2000.
- Nakanishi, M., Topographic expression of five fracture zones in the northwestern Pacific Ocean, in *The Mesozoic Pacific: Geology, Tectonics, and Volcanism, Geophys. Monogr. Ser.*, vol. 77, edited by M. S. Pringle et al., pp. 121–136, AGU, Washington, D. C., 1993.
- Nakanishi, M., K. Tamaki, and K. Kobayashi, Magnetic anomaly lineations from late Jurassic to Early Cretaceous in the west-central Pacific Ocean, *Geophys. J. Int.*, 144, 535–545, 1992.
- Phipps Morgan, J., Thermodynamics of pressure release melting of a veined plum pudding mantle, *Geochem. Geophys. Geosyst.*, 2, paper number 2000GC000049, 2001.
- Phipps Morgan, J., and W. J. Morgan, Two-stage melting and the geochemical evolution of the mantle: A recipe for mantle plum-pudding, *Earth Planet. Sci. Lett.*, 170, 215–239, 1999.
- Plank, T., et al., *Proceedings of the Ocean Drilling Program, Initial Reports*, vol. 185, Ocean Drill. Program, College Station, Tex., 2000.
- Pockalny, R. A., and R. L. Larson, Implications for crustal accretion at fast spreading ridges from observations in Jurassic oceanic crust in the western Pacific, *Geochem. Geophys. Geosyst.*, 4(1), 8903, doi:10.1029/2001GC000274, 2003.
- Pringle, M. S., Radiometric ages of basaltic basement recovered at Sites 800, 801, and 802, Leg 129, Western Pacific ocean, *Proc. Ocean Drill. Program Sci. Results*, 129, 389–404, 1992.
- Pringle, M. S., L. M. Chambers, and J. Ogg, Synchronicity of volcanism on Ontong Java and Manihiki plateaux with global oceanographic events?, paper presented at New Frontiers in the Fourth Dimension: Generation, Calibration and Application of Geological Timescales: NUNA Conference, Geol. Assoc. of Canada, Mont Tremblant, Quebec, Canada, 15 – 18 March 2003.
- Renne, P. R., A. L. Deino, R. C. Walter, B. D. Turrin, C. C. Swisher III, T. A. Becker, G. H. Curtis, W. D. Sharp, and A.-R. Jaouni, Intercalibration of astronomical and radioisotopic time, *Geology*, 22, 783–786, 1994.
- Renne, P. R., C. C. Swisher, A. L. Deino, D. B. Karner, T. L. Owens, and D. J. DePaolo, Intercalibration of standards, absolute ages and uncertainties in $^{40}\text{Ar}/^{39}\text{Ar}$ dating, *Chem. Geol.*, 145, 117–152, 1998.
- Renne, P. R., R. Mundil, and K. R. Ludwig, Outstanding problems in the geochronological calibration of the timescale, paper presented at New Frontiers in the Fourth Dimension: Generation, Calibration and Application of Geological Timescales: NUNA Conference, Geol. Assoc. of Canada, Mont Tremblant, Quebec, Canada, 15 – 18 March 2003.

- Schmitz, M. D., and S. A. Bowring, U-Pb zircon and titanite systematics of the Fish Canyon Tuff: An assessment of high-precision U-Pb geochronology and its application to young volcanic rocks, *Geochim. Cosmochim. Acta*, *65*, 2571–2587, 2001.
- Spell, T. L., and I. McDougall, Characterization and calibration of ⁴⁰Ar/³⁹Ar dating standards, *Chem. Geol.*, *198*, 189–211, 2003.
- Steiger, R. H., and E. Jäger, Subcommittee on geochronology: Convention on the use of decay constant in geo- and cosmochronology, *Earth Planet. Sci. Lett.*, *36*, 359–362, 1977.
- Stoenner, R. W., O. A. Schaeffer, and S. Katcoff, Half-lives of argon-37, argon-39 and argon-42, *Science*, *148*, 1325–1328, 1965.
- Taylor, J. R., *An Introduction to Error Analysis: The Study of Uncertainties in Physical Measurements*, 327 pp., Univ. Sci. Books, Mill Valley, Calif., 1997.
- Weast, R. C., *Handbook of Chemistry and Physics*, 62nd ed. CRC Press, Boca Raton, Fla., 1981.
- Wijbrans, J. R., M. S. Pringle, A. A. P. Koppers, and R. Scheveers, Argon geochronology of small samples using the Vulkan argon laserprobe, *Proc. K. Ned. Akad. Wet. Biol. Chem. Geol. Phys. Med. Sci.*, *98*, 185–218, 1995.
- York, D., Least squares fitting of a straight line with correlated errors, *Earth Planet. Sci. Lett.*, *5*, 320–324, 1969.
- Zindler, A., H. Staudigel, and R. Batiza, Isotope and trace element geochemistry of young Pacific seamounts: Implications for the scale of upper mantle heterogeneity, *Earth Planet. Sci. Lett.*, *70*, 175–195, 1984.